Metal aluminum amides for hydrogen storage – crystal structure studies

Satoshi Hino[a], Hilde Grove[a], Takayuki Ichikawa[b], Yoshitsugu Kojima[b], Magnus H. Sørby[a,*], Bjørn C. Hauback[a]

[a] Physics Department, Institute for Energy Technology, P.O. Box 40, NO-2027 Kjeller, Norway

[b] Institute for Advanced Materials Research, Hiroshima University, 1-3-1 Kagamiyama, Higashi-Hiroshima, 739-8530, Japan.

* Corresponding author. Tel.: +47 6380 6499; fax: +47 6381 0920. E-mail address: magnuss@ife.no (M. H. Sørby).

Abstract

Crystal structure of metal aluminum amides has been investigated by synchrotron radiation powder X-ray diffraction (SR-PXD) and powder neutron diffraction (PND). Alkali and alkaline-earth metal aluminum amides $M[Al(NH_2)_4]_x$ desorb ammonia during thermal decomposition and have recently been studied as possible hydrogen storage system by making composites with metal hydrides. In this work, deuterated metal aluminum amides $M[Al(ND_2)_4]_x$ with M = Li, Na, K, Mg and Ca were synthesized by ball-milling of M (or MD_x) + Al (or AlD_3) under liquid ND_3. The crystal structures of $MAl(ND_2)_4$ phases with M = Li, Na, K (α-phase) have been refined by simultaneous Rietveld refinement using PND and SR-PXD data. Structure determination was successful for β-$KAl(ND_2)_4$ and $Ca[Al(ND_2)_4]_2$. The structures are composed of $[Al(ND_2)_4]^-$ tetrahedra and M cations, and the unit cells are: M = Li; monoclinic space group $P2_1/n$, a = 9.5075(3) Å, b = 7.3610(2) Å, c = 7.4076(2) Å, β = 90.165(3)°, Na; monoclinic space group $P2_1/c$, a = 7.3317(9) Å, b = 6.0447(8) Å, c = 13.151(2) Å, β = 94.110(9)°, K (α-phase); orthorhombic space group $C222_1$, a = 10.17258(7) Å, b = 5.78762(5) Å, c = 9.98651(7) Å, K (β-phase); orthorhombic space group *Pnma*, a = 11.4183(4) Å, b = 8.8588(2) Å, c = 6.1696(2) Å, and Ca; monoclinic space group *Pc*, a = 6.4321(2) Å, b = 6.4377(2) Å, c = 12.2939(3) Å, β = 90.612(2)°. The structural features of metal aluminum amides have been compared with the corresponding alanates.

Keywords: Hydrogen storage materials, Powder neutron diffraction, Powder X-ray diffraction, Ball-milling

Introduction

Utilization of hydrogen as an energy carrier is one of the key challenges in developing a carbon-neutral energy economy. Compact and safe way to store hydrogen is necessary [1], and one of the candidates is hydrogen storage in solid materials which possess high volumetric hydrogen capacity. Complex hydrides, e.g., metal alanates $M(AlH_4)_x$ where hydrogen is covalently bonded with Al to make complex anion, have high gravimetric hydrogen capacity and have been studied as one of the most promising hydrogen storage materials [2]. For example, $LiAlH_4$ can store 10.5 mass% hydrogen, however the irreversibility of the hydrogen desorption reaction is challenging. $NaAlH_4$ with transition metal additives shows good cyclability, however the practical reversible capacity is only around 4 wt% H [3].

Metal aluminum amides (tetra-amido-aluminates), $M[Al(NH_2)_4]_x$, consist of complex ion of Al tetrahedrally coordinated by four NH_2^-, $Al(NH_2)_4^-$ and balancing alkali or alkaline-earth metal cations, M^{x+}. They can thus be regarded as metal alanates where the hydrogen atoms have been substituted by NH_2. The compounds desorb NH_3 during thermal decomposition and the NH_3 desorption properties have been investigated with temperature-programmed-desorption coupled with a mass spectrometer (TPD-MS), and it reveals that the main NH_3 release occurs in the range 50 - 150 °C for $M[Al(NH_2)_4]_x$ (M = Li, Na, K, Mg and Ca) [4, 5]. Analogously to the amide-imide system [6], NH_3 desorption in metal aluminum amides can be replaced by H_2 desorption by making composites with alkali metal hydrides, therefore the compounds have recently been studied as hydrogen storage materials. The lithium amide-imide system desorbs ~6.5 mass% H_2 at 255 °C through the following reaction: [6]

$$LiNH_2 + LiH \rightarrow Li_2NH + H_2$$

For more unstable amides the H_2 desorption temperature is decreased, e.g., the composite LiH-$LiAl(NH_2)_4$ can desorb up to 6.2 mass% hydrogen at 130 °C [7].

The reactions between Al and solution of alkali metals (Li, Na, K, Rb and Cs) in liquid NH_3 result in single crystals of the alkali metal aluminum amides and the unit cell parameters of these compounds have been investigated by powder and single crystal diffraction [8-10]. The crystal structures of $LiAl(NH_2)_4$, $NaAl(NH_2)_4$, α-$KAl(NH_2)_4$, $RbAl(NH_2)_4$ and $CsAl(NH_2)_4$ have

been reported from single crystal X-ray diffraction measurements [11-14]. The structure models included hydrogen positions, but they are regarded as uncertain due to their low X-ray scattering power. The space groups and unit cell parameters of $MAl(NH_2)_4$ for M = Li, Na, α-K, Rb and Cs respectively, are $P2_1/n$, a = 9.478(1) Å, b = 7.351(1) Å, c = 7.398(1) Å, β = 90.268(1)°; and $P2_1/c$, a = 7.328(2) Å, b = 6.047(2) Å, c = 13.151(3) Å, β = 94.04°; and $C222_1$, a = 10.00(1) Å, b = 5.80(1) Å, c = 10.14(1) Å; and $P4/n$, a = 7.406(4) Å, c = 5.386(4) Å; and $P4/n$, a = 7.563(3) Å, c = 5.354(1) Å. The crystal structure data are summarized in Table 1 together with those of other known metal aluminum amides and related compounds. Brec and Rouxel [10] have reported the space group and unit cell parameters of β-$KAl(NH_2)_4$: *Pnma*, a = 11.37(1) Å, b = 8.85(1) Å, c = 6.146(6) Å but without atomic positions. Recently, a study on structures and bonding of alkali metal aluminum amides investigated by IR spectroscopy supported by DFT calculations has been reported [4]. For group 2 elements, the crystal structures of $Mg[Al(NH_2)_4]_2$ and $Ca[Al(NH_2)_4]_2$ are unknown except for their unit cell parameters: hexagonal (a = 12.10 Å and c = 7.95 Å) and monoclinic (a = 12.27 Å, b = 6.44 Å, c = 6.43 Å, and β = 90.7°) unit cells, respectively [5]. Furthermore $Sr[Al(NH_2)_4]_2$ and $Ba[Al(NH_2)_4]_2$ have been synthesized [15]. The unit cell parameters of $Sr[Al(NH_2)_4]_2$ were determined (hexagonal, a = 17.49(1) Å, c = 28.17(2) Å), but $Ba[Al(NH_2)_4]_2$ was unstable at ambient conditions without ammonia pressure. Recently, low-temperature single crystal measurement has revealed crystal structure of $Ba(Al(NH_2)_4)_2 \cdot 2NH_3$ synthesized by an ammonothermal method [16].

Table 1. Crystal structure data of metal aluminum amides and related compounds. Lattice constants (*a*, *b*, *c* and *β*), unit cell volume (*V*) and formula units per unit cell (*Z*). "*" denotes compounds where atomic positions have been reported. Estimated standard deviations are given in parentheses when reported.

Compound	Space group	*a* / Å	*b* / Å	*c* / Å	*β* (°)	*V* / Å^3	*Z*	Ref.
$LiAl(NH_2)_4$	$P2_1/n$	9.478(1)	7.351(1)	7.398(1)	90.26(1)	519.39	4	[11] *
$NaAl(NH_2)_4$	$P2_1/c$	7.328(2)	6.047(2)	13.151(3)	94.04(1)	581.3	4	[12] *
$Na_2Al(NH_2)_5$	*Cmma* or *Abm*2	23.56	19.36	6.78	90	3092.5	16	[17]
α-$KAl(NH_2)_4$	$C222_1$	10.00(1)	5.80(1)	10.14(1)	90	588.12	4	[13] *
β-$KAl(NH_2)_4$	*Pnma*	11.37(1)	8.85(1)	6.146(6)	90	618.44	4	[10]
$RbAl(NH_2)_4$	*P*4/*n*	7.406(4)	7.406(4)	5.386(4)	90	295.42	2	[14] *
$CsAl(NH_2)_4$	*P*4/*n*	7.563(3)	7.563(3)	5.354(1)	90	306.24	2	[14] *
$Mg(Al(NH_2)_4)_2$	Hexagonal	12.1	12.1	7.95	90	1008.02	N/A	[5]
$Ca(Al(NH_2)_4)_2$	Monoclinic	12.27	6.44	6.43	90.7	508.05	N/A	[5]
$Ca(Al(NH_2)_4)_2{\cdot}NH_3$	*I*2/*c*	10.189(9)	9.897(11)	12.151(12)	98.60(15)	1211.54	4	[18] *
$CaAl(NH_2)_5$	$P4_222$	6.471(5)	6.471(5)	12.244(9)	90	512.70	4	[19]
$Sr(Al(NH_2)_4)_2$	$P6_2$, $P6_4$, $P6_222$, or $P6_422$	17.49(1)	17.49(1)	28.17(2)	90	7462.72	36	[15]
$Ba(Al(NH_2)_4)_2{\cdot}2NH_3$	*R*-3*c*	15.7370(17)	15.7370(17)	28.840(6)	90	6177.71	18	[16] *

In the present work, deuterated metal aluminum amides $M[Al(ND_2)_4]_x$, with M = Li, Na, K, Mg and Ca, were synthesized, and their crystal structures were investigated using both powder neutron diffraction (PND) and synchrotron radiation powder X-ray diffraction (SR-PXD).

Experimental

The starting materials LiD (98% purity), $LiAlD_4$ (95%), $AlCl_3$ (99.999%) and elemental Na (99.95%), K (99.95%) and Ca (99.99%) were obtained from Sigma-Aldrich Co., Al (99.9%, 3 μm) from Rare metallic co. Ltd. and Mg (99.99%, #200) from Kojundo Chemical Lab. Co. Ltd. In the preparation of the metal deuterides, Na or K were annealed under D_2 atmosphere (1 MPa) at 650 °C for 20 h and Ca at 300 °C for 8 h. AlD_3 was prepared from the reaction between $LiAlD_4$ and $AlCl_3$ by wet chemistry [20]. The starting materials for each metal aluminum amide listed in Table 2 were loaded into Cr-steel vials (SDK-11, UMETOKU Co. Ltd.) with ZrO_2 balls and milled with sequences of 15 min mill followed by 15min pause under liquid ND_3 or gaseous argon by using a rocking mill apparatus (RM-10, SEIWA GIKEN Co. Ltd.) with a frequency of 10 Hz. The detailed milling conditions are described in Table 2. All handling of samples was carried out in a glove box filled with purified argon (<1 ppm O_2 and H_2O).

Table 2. Summary of experimental conditions for the ball-milling to synthesize the metal aluminum amides.

	Milled materials	Molar ratio	Milling atmosphere	Milling time[a]	Additional treatment
$LiAl(ND_2)_4$	LiD + Al	1 : 1	Ar (1 MPa)	20 h	Annealing under liq. ND_3 at 100 °C for 2 weeks
$NaAl(ND_2)_4$	NaD + AlD_3	1 : 1	Liq. ND_3	4 h	Kept for 1 week under liq. ND_3 at RT
$KAl(ND_2)_4$	KD + AlD_3	1 : 1	Liq. ND_3	4 h	Kept for 1 week under liq. ND_3 at RT
$Mg[Al(ND_2)_4]_2$	Mg + Al	1 : 2	Liq. ND_3	8 h	Kept for 1 week under liq. ND_3 at RT
$Ca[Al(ND_2)_4]_2$	CaD_2 + Al	1 : 2	Liq. ND_3	10 h	Kept for 1 week under liq. ND_3 at RT

[a] Active milling time (without pauses).

In situ SR-PXD measurements were carried out using a pixel area detector (Pilatus2M, DECTRIS) at the Swiss-Norwegian Beamline (SNBL, BM01A) at the European Synchrotron Radiation Facility (ESRF), Grenoble, France. The samples were mounted in boron glass capillaries (0.5 mmϕ) fixed in a Swagelok fitting and kept under dynamic vacuum. A diffraction pattern was collected every 40 s (exposure time 30 s). The capillary was rotated 30° during exposure to improve the powder averaging. Measurements were carried out between room temperature (RT) and 500 °C. The two-dimensional data were integrated to one-dimensional diffraction patterns using the Fit2D program [21].

High resolution SR-PXD data at RT were collected at SNBL, BM01B at ESRF, Grenoble, France. The diffractometer is equipped with six scintillation detectors mounted with 1.1° separation in 2θ, each with a secondary Si monochromator. The samples were filled and sealed in boron glass capillaries (0.5 mmϕ) under Ar atmosphere and placed on a spinning stage.

PND data were collected at the JEEP II reactor at Kjeller, Norway, with the PUS instrument [22]. Neutrons with wavelength 1.5556 Å were obtained from a Ge (511) focusing monochromator. The detector unit consists of two banks of seven position-sensitive ^{3}He detectors, each covering 20° in 2θ (binned in steps of 0.05°). Diffraction data were collected at RT from 10 to 130° in 2θ. The sample was kept in a rotating cylindrical vanadium sample holder (6 mmϕ).

The Dicvol [23] and Chekcell [24] programs were used for unit cell and space group determination. The global optimization approach with parallel tempering as implemented in the FOX program [25, 26] was used for crystal structure determination. The structure refinements were carried out using the GSAS [27] software package with the EXPGUI [28] user interface based on the Rietveld method [29, 30]. The backgrounds were fitted with a 24-term shifted-Chebyshev polynominals (M = Li, α-K, Ca) or by interpolation between manually selected points (M = Na, β-K). A pseudo-Voigt function [31] with asymmetry correction [32] was used to model the peak profile. Isotropic thermal displacement parameters were refined with a common U_{iso} value for D-atoms in $LiAl(ND_2)_4$, $NaAl(ND_2)_4$, α-$KAl(ND_2)_4$ and $Ca[Al(ND_2)_4]_2$, and for N-atoms in $NaAl(ND_2)_4$ and β-$KAl(ND_2)_4$, respectively. Interatomic distance restraints were employed as follows: Al-N distances in each $Al(ND_2)_4$ unit were 1.85 Å in $NaAl(ND_2)_4$ and β-$KAl(ND_2)_4$ and N-D distances 1.0 Å in $NaAl(ND_2)_4$ and $Ca[Al(ND_2)_4]_2$. The restraint weight factor of 5000 was applied which gave a minimal impact on the R-factors. The crystal structures were illustrated using the VESTA program [33].

Fourier transform infrared (FTIR) spectrometer (ALPHA, Bruker) equipped with a 45° diamond attenuated total reflectance (ATR) accessory was used to collect IR spectra at RT. The spectrometer was installed in a glove box filled with purified Ar.

Results and discussion

Fig. S1 shows SR-PXD profiles for all the synthesized $M[Al(ND_2)_4]_x$ samples. They are in good agreement with X-ray diffraction data for $M[Al(NH_2)_4]_x$ reported in previous studies [4, 5], suggesting that the syntheses of the deuterated materials were successful. According to the literature [10], $KAl(NH_2)_4$ takes two structure modifications, α and β, and our synthesized $KAl(ND_2)_4$ exhibits the α-phase. Traces of unreacted aluminum metal were detected in the $Mg[Al(ND_2)_4]_2$ and $Ca[Al(ND_2)_4]_2$ samples. The $KAl(ND_2)_4$ sample contained a minor amount of partially decomposed product $KAl(ND_2)_2ND$ and unreacted KD.

Fig. 1 shows infrared spectra for N-D stretching mode of $M[Al(ND_2)_4]_2$ measured at RT. The observed N-D absorption peak profiles are in good agreement with the N-H absorption bands in $M[Al(ND_2)_4]_x$ as reported in the previous works [4, 5] with the expected shift due to the isotope effect when replacing H with D [34]. Amide ions have symmetric and asymmetric stretching modes, which provide two absorption bands in the IR spectra.

In-situ SR-PXD measurements were carried out for the as-synthesized materials. Previous studies revealed that $LiAl(NH_2)_4$ transforms into an amorphous intermediate phase $LiAl(NH_2)_x(NH)_yN_z$ during thermal decomposition [35]. Our *in-situ* SR-PXD data of all samples are shown in Fig. 2. The crystalline metal aluminum amides became amorphous at around 137, 103, 141, and 130 °C for *M* = Li, Na, Mg, and Ca, respectively. In the case of $KAl(ND_2)_4$, the phase transformation from α to β was observed at around 60 °C, and the β-phase disappeared at around 66 °C as shown in Fig.2c. These amorphization temperatures are consistent with ammonia desorption temperatures of metal aluminum amides determined from thermal desorption mass spectroscopy [5].

To determine the deuterium positions of $LiAl(ND_2)_4$, $NaAl(ND_2)_4$ and α-$KAl(ND_2)_4$, simultaneous SR-PXD and PND Rietveld refinements were performed for these samples using the previously reported structure models [11-13] as initial parameters. The results of the Rieveld refinements based on both the SR-PXD and PND data for $LiAl(ND_2)_4$, $NaAl(ND_2)_4$ and α-$KAl(ND_2)_4$ are shown in Fig. 3a-3c and 4a-4c, respectively. Because $NaAl(ND_2)_4$ shows a preferential (002) plane orientation compared to the previously reported model, March-Dollase correction was applied. The refinement results are summarized in Table 3-5 and the structure

models are illustrated in Fig. S2-S4. The refined crystal structures are in good agreement with the previously reported structure models.

Table 3. Results from simultaneous PND and SR-PXD Rietveld refinement of $LiAl(ND_2)_4$. R_{wp} = 3.57% for PND, R_{wp} = 4.48% for SR-PXD. Estimated standard deviations are in parentheses.

Space group: $P2_1/n$ (No. 14), Z = 4, T = 22 °C a = 9.5075(3) Å, b = 7.3610(2) Å, c = 7.4076(2) Å, β = 90.165(3)°					
Atom	Site	x	y	z	U_{iso} / Å^2
Al	4*e*	0.8582(3)	0.2481(12)	0.0060(9)	0.0262(10)
N1	4*e*	0.5256(4)	0.7533(8)	0.2967(7)	0.0282(11)
N2	4*e*	0.7549(7)	0.4687(7)	-0.0014(8)	0.0513(17)
N3	4*e*	0.4637(5)	0.2331(8)	0.2976(8)	0.0458(16)
N4	4*e*	0.2280(5)	0.4439(6)	0.4716(7)	0.0306(12)
Li	4*e*	0.1215(17)	0.4838(18)	0.2379(17)	0.005(3)
D1	4*e*	0.5645(8)	0.7647(13)	0.1799(14)	0.0621(8)
D2	4*e*	0.4645(9)	0.6381(13)	0.2750(12)	0.0621(8)
D3	4*e*	0.6638(10)	0.4489(13)	0.0133(13)	0.0621(8)
D4	4*e*	0.7553(10)	0.5408(11)	0.1171(13)	0.0621(8)
D5	4*e*	0.5660(7)	0.2404(14)	0.3024(11)	0.0621(8)
D6	4*e*	0.4203(8)	0.3030(10)	0.1824(15)	0.0621(8)
D7	4*e*	0.2710(9)	0.5685(10)	0.4979(14)	0.0621(8)
D8	4*e*	0.1534(11)	0.4362(12)	0.5675(10)	0.0621(8)

Table 4. Results from simultaneous PND and SR-PXD Rietveld refinement of $NaAl(ND_2)_4$. R_{wp} = 8.50% for PND, R_{wp} = 11.39% for SR-PXD. Estimated standard deviations are in parentheses.

Space group: $P2_1/c$ (No. 14), Z = 4 , T = 22 °C a = 7.3317(9) Å, b = 6.0447(8) Å, c = 13.151(2) Å, β = 94.110(9)°					
Atom	Site	x	y	z	U_{iso} / Å^2
Al	4*e*	0.2318(15)	0.1587(18)	0.1607(7)	0.049(5)
Na	4*e*	0.7307(18)	0.161(2)	0.1889(10)	0.067(6)
N1	4*e*	0.4404(10)	0.2306(16)	0.0937(6)	0.0231(4)
N2	4*e*	0.2992(10)	0.2387(18)	0.2868(7)	0.0231(4)
N3	4*e*	0.0029(11)	0.2606(15)	0.0957(5)	0.0231(4)
N4	4*e*	0.7542(12)	0.3397(12)	0.3457(7)	0.0231(4)
D1	4*e*	0.444(3)	0.378(3)	0.0721(16)	0.098(2)
D2	4*e*	0.556(3)	0.771(4)	0.9828(12)	0.098(2)
D3	4*e*	0.424(2)	0.235(4)	0.3296(12)	0.098(2)
D4	4*e*	0.795(2)	0.753(4)	0.1610(14)	0.098(2)
D5	4*e*	0.988(2)	0.330(3)	0.1687(13)	0.098(2)
D6	4*e*	0.049(2)	0.752(4)	0.4817(12)	0.098(2)
D7	4*e*	0.750(3)	0.303(4)	0.4222(12)	0.098(2)

D8	4*e*	0.889(2)	0.281(3)	0.3639(16)	0.098(2)

Table 5. Results from simultaneous PND and SR-PXD Rietveld refinement of α-$KAl(ND_2)_4$. R_{wp} = 5.56% for PND, R_{wp} = 9.43% for SR-PXD. Estimated standard deviations are in parentheses.

Space group: $C222_1$ (No. 20), Z = 4, T = 22 °C a = 10.17258(7) Å, b = 5.78762(5) Å, c = 9.98651(7) Å					
Atom	Site	*x*	*y*	*z*	U_{iso} / Å^2
K	4*a*	0.24249(19)	0	0	0.0457(7)
Al	4*b*	0	0.4433(4)	0.25	0.0280(7)
N1	8*c*	0.3606(3)	0.1416(6)	0.2788(4)	0.0338(12)
N2	8*c*	-0.0108(5)	0.2506(5)	0.1056(3)	0.0320(12)
D1	8*c*	0.2238(14)	0.598(2)	0.1936(14)	0.059(3)
D2	8*c*	0.1340(9)	0.778(3)	0.2560(18)	0.059(3)
D3	8*c*	0.4622(14)	0.405(3)	0.8937(12)	0.059(3)
D4	8*c*	0.5142(15)	0.210(2)	0.9808(12)	0.059(3)

Based on the SR-PXD data, β-$KAl(ND_2)_4$ can be indexed with an orthorhombic unit cell with a = 11.4183(4) Å, b = 8.8588(2) Å, c = 6.1696(2) Å. This is almost the same unit cell as in the earlier study and the systematic extinctions are in agreement with the suggested space group *Pnma* [10]. The atomic positions of K, Al and N, were determined from the SR-PXD data measured at around 60 °C. Fig. 3d shows obtained Rietveld fit of β-$KAl(ND_2)_4$ to the SR-PXD data. Refined structure parameters are listed in Table 6 and the structure model is illustrated in Fig. 5.

Table 6. Results from SR-PXD Rietveld refinement of β-$KAl(ND_2)_4$ (R_{wp} = 4.80%). Estimated standard deviations are shown in parentheses.

Space group: *Pnma* (No. 62), Z = 4, T = 60 °C, a = 11.4183(4) Å, b = 8.8588(2) Å, c = 6.1696(2) Å					
Atom	Site	*x*	*y*	*z*	U_{iso} / Å^2
K	4*c*	0.3555(5)	0.25	0.5914(8)	0.026(2)
Al	4*c*	0.1868(5)	0.25	0.0528(10)	0.003(2)
N1	8*d*	0.3455(8)	0.25	0.056(3)	0.056(4)
N2	4*c*	0.0967(13)	0.25	0.801(2)	0.056(4)
N3	4*c*	0.1479(9)	0.0891(9)	0.2321(13)	0.056(4)

The SR-PXD and PND patterns of $Mg[Al(ND_2)_4]_2$ show rather broad and asymmetric peaks (Fig. S5). The peak positons are in fair agreement with the previously suggested hexagonal unit cell with a = 12.09 and c = 7.968 Å [5]. SR-PXD data gives the unit cell parameters a = 12.08 and c = 7.974 Å and possible space group $P6$, however, it has not succeeded to solve the structure based on these data.

To our best knowledge, no structure model of $Ca[Al(NH_2)_4]_2$ has been reported earlier. Indexing of the PXD diagram of $Ca[Al(ND_2)_4]_2$ gives a monoclinic unit cell with parameters a = 6.4321(2) Å, b = 6.4377(2) Å, c = 12.2939(3) Å, β = 90.612(2)°, and space group of Pc. These values are in good agreement with the previously reported unit cell parameters (a = 12.27 Å, b = 6.44 Å, c = 6.43 Å, and β = 90.7°) [5]. Atomic positions were determined from SR-PXD and PND data using the program FOX and the fits obtained by Rietveld refinement are shown in Fig. 3e and 4d. By analogy to known structures of $MAl(ND_2)_4$, Al atoms tetrahedrally coordinated by ND_2 units were considered to build structure model of $Ca[Al(ND_2)_4]_2$. Fig. 6 shows the refined structure and the crystallographic data are presented in Table 7.

Table 7. Results from simultaneous PND and SR-PXD Rietveld refinement of $Ca[Al(ND_2)_4]_2$. R_{wp} = 3.30% for PND, R_{wp} = 8.91% for SR-PXD. Estimated standard deviations are given in parentheses.

Space group: *Pc* (No. 7), *Z* = 2, *T* = 22 °C *a* = 6.4321(2) Å, *b* = 6.4377(2) Å, *c* = 12.2939(3) Å, *β* = 90.612(2)°					
Atom	Site	*X*	*y*	*z*	U_{iso} / Å^2
Ca	2*a*	0.4578(11)	0.6768(5)	0.1704(5)	0.0327(10)
Al1	2*a*	0.5043(15)	0.4400(8)	0.4173(7)	0.031(2)
Al2	2*a*	0.0081(14)	0.0887(7)	0.6320(7)	0.038(3)
N1	2*a*	0.5269(17)	0.3863(16)	0.0401(8)	0.031(3)
D1	2*a*	0.672(3)	0.328(4)	0.052(3)	0.066(2)
D2	2*a*	0.435(4)	0.257(4)	0.040(3)	0.066(2)
N2	2*a*	0.2613(17)	0.5211(16)	0.3394(8)	0.032(3)
D3	2*a*	0.191(4)	0.389(4)	0.3168(17)	0.066(2)
D4	2*a*	0.203(4)	0.652(4)	0.3716(18)	0.066(2)
N3	2*a*	0.4860(16)	0.1732(14)	0.4770(8)	0.025(3)
D5	2*a*	0.622(4)	0.102(5)	0.469(2)	0.066(2)
D6	2*a*	0.358(4)	0.086(4)	0.481(3)	0.066(2)
N4	2*a*	0.7097(16)	0.4683(16)	0.3169(9)	0.033(3)
D7	2*a*	0.774(4)	0.335(4)	0.286(2)	0.066(2)
D8	2*a*	0.830(4)	0.558(4)	0.329(3)	0.066(2)
N5	2*a*	0.0709(17)	0.6459(14)	0.0950(8)	0.032(3)
D9	2*a*	0.051(5)	0.588(4)	0.0219(14)	0.066(2)
D10	2*a*	0.006(4)	0.529(3)	0.1327(17)	0.066(2)
N6	2*a*	0.2317(18)	0.0057(15)	0.2138(9)	0.037(3)
D11	2*a*	0.330(4)	0.124(4)	0.204(3)	0.066(2)
D12	2*a*	0.214(5)	0.025(5)	0.2915(14)	0.066(2)
N7	2*a*	0.7473(18)	0.0776(16)	0.7046(9)	0.049(4)
D13	2*a*	0.693(4)	0.061(3)	0.177(3)	0.066(2)
D14	2*a*	0.730(4)	0.064(4)	0.7849(14)	0.066(2)
N8	2*a*	0.000(3)	0.0690(18)	0.0000(9)	0.080(5)
D15	2*a*	0.031(5)	0.224(3)	0.0133(18)	0.066(2)
D16	2*a*	0.949(5)	0.005(4)	0.4337(16)	0.066(2)

Selected interatomic distances in $M[Al(NH_2)_4]_2$ are summarized in Table 8 and details are shown in Table S1-S5. It is found that M-N and Al-N distances show a good agreement with the previously reported values for $MAl(NH_2)_4$, however, N-D distances are significantly longer than N-H distances. In general X-ray diffraction experiments tend to give short metal-hydrogen distances, because of its sensitivity to electrons rather than the atomic nucleus. These trends have also been found in the metal amide system, e.g., N-D distances from PND (0.99 and 1.00 Å) in

$LiND_2$ are longer than N-H distances (0.70 and 0.76 Å) from PXD in $LiNH_2$ [36, 37]. In addition, DFT calculations predicted a N-H distance of 1.03 Å [38]. In case of $Ca[Al(ND_2)_4]_2$, it is reported that $CaAl_2(NH_2)_8NH_3$ (space group *I*2/*c*, *a* = 10.189(9) Å, *b* = 9.897(11) Å, *c* = 12.151(12) Å, and β = 98.36(9)°) has Ca-N distance (mean value) of 2.60 Å between Ca^{2+} and N in $Al(NH_2)_4^-$ tetrahedra, and Al-N mean distance of 1.85 Å in the tetrahedral [18]. These values are consistent with the distances Ca-N = 2.475(11)-2.758(10) Å, Al-N = 1.815(10)-1.914(12) Å and N-D = 0.971(13)-1.033(13) Å obtained here for $Ca[Al(ND_2)_4]_2$. Similarly, the N-H distances of the amide ions in $CaAl_2(NH_2)_8NH_3$ is also underestimated, mean value: 0.89 Å, from single crystal X-ray diffraction.

Table 8. Mean values of interatomic distances (Å) and bond angles (°) for $M[Al(ND_2)_4]_x$ from the Rietveld refinements. The values are compared with published data based from $MAl(NH_2)_4$ based on PXD data. Standard deviations are given in parentheses.

	This work				Reference				
M	M-N	Al-N	N-D	D-N-D	M-N	Al-N	N-H	H-N-H	
Li	2.023(15)-2.213(15)	1.830(7)-1.898(9)	0.886(9)-1.078(10)	98.7(9)-112.5(9)	2.059(8)-2.191(8)	1.840(4)-1.867(3)	0.71(5)-0.94(4)	89.1(13)-105.4(10)	[11]
Na	2.324(15)-2.582(16)	1.763(11)-1.933(11)	0.936(14)-1.063(13)	72.8(19)-146.7(19)	2.446(3)-2.480(3)	1.842(3)-1.855(3)	0.69(3)-0.87(3)	102.0(10)-105.5(10)	[12]
α-K	3.082(5)-3.207(4)	1.827(3), 1.847(3)	0.865(16)-0.940(15)	109.0 (11), 115.2(11)	3.052(12)-3.246(16)	1.801(10)-1.887(17)	0.66(15)-0.9(2)	116(3)	[13]
β-K	2.832(14)-3.305(16)	1.812(7)-1.863(7)	-	-	-	-	-	-	
Ca	2.475(11)-2.758(10)	1.815(10)-1.914(12)	0.971(13)-1.033(13)	95(2)-130(3)	-	-	-	-	

Metal aluminum amides are analogous compounds of metal alanates where the H in AlH_4 tetrahedra are substituted by NH_2. However, the crystal structures of metal aluminum amides are typically different from the corresponding metal alanates. The differences and similarities of the crystal structures between metal aluminum amides and corresponding metal alanates will be discussed below. Coordination of metal cation to AlD_4 in metal alanates or to $Al(ND_2)_4$ in metal aluminum amides is illustrated in Fig. 7. While the alkali cations have coordination numbers 5 and 8 in $LiAlD_4$ and $NaAlD_4$, respectively [39, 40], the cation is tetrahedrally coordinated by

$Al(ND_2)_4$ ions (coordination number 4) in $LiAl(ND_2)_4$ and $NaAl(ND_2)_4$. The NaN_4 tetrahedra in the latter are connected to four different AlN_4 tetrahedra by corner sharing. The LiN_4 tetrahedra in $LiAl(ND_2)_4$ are connected to four N atoms from three AlN_4 sharing two vertices and one edge from three AlN_4. For α-$KAl(ND_2)_4$, K atom is surrounded by eight N atoms in a distorted square antiprismatic configuration sharing four vertices and two edges from six AlN_4 tetrahedra. This coordination is similar to that of $NaAlD_4$ and $Ca(AlD_4)_2$ [41, 42]. In the β-phase, the K atom has coordination number 6 with five AlN_4 tetrahedra (four vertices and one edge). The Ca atom in $Ca[Al(ND_2)_4]_2$ is surrounded by seven N atoms from four different AlN_4 sharing one vertices and three edges.

Table 9 summarizes selected interatomic distances and bond angles in metal alanates and aluminum amides. Fig. 8 shows the average M-D or M-N distances in $M[AlD_4]_x$ or $M[Al(ND_2)_4]_x$, respectively, as a function of effective ionic radii of the metal [43]. For the alanates, larger cation results in a longer cation-D distance [42], which is also the case for the cation-N distances in aluminum amides. These distances show linear correlation with effective ionic radii. The intercepts of the linear fits are 1.14 and 1.35 Å, respectively, which is in good agreement with the reported effective ionic radii of H^- (1.22 Å) and N^{3-} (1.46 Å) [43].

Table 9. Coordination numbers (CN) of M and selected interatomic distances (Å) and bond angles (°) in metal alanates $M(AlD_4)_x$ from the literatures and metal aluminum amides $M[Al(ND_2)_4]_x$ (M = Li, Na, K and Ca) from this work. Standard deviations are given in parentheses.

	Alanates $M(AlD_4)_x$					Aluminum amides $M[Al(ND_2)_4]_x$				
	Li [39]	Na [40]	K [44]	Ca [42]		Li	Na	K (α-phase)	K (β-phase)	Ca
CN	5	8	10	8		4	4	8	6	7
Al-D	1.605(6) 1.633(5) 1.623(5) 1.603(7)	4× 1.626(2)	1.546(13) 1.669(13) 2× 1.629(8)	1.605(6), 1.604(6) 1.598(6), 1.603(6) 1.619(6), 1.621(6) 1.639(5), 1.603(6)	Al−N	1.830(7) 1.898(9) 1.849(8) 1.895(8)	1.919(11) 1.814(11) 1.848(11) 1.901(11)	2× 1.847(3) 2× 1.827(3)	1.812(7) 1.863(7) 2× 1.858(5)	1.884(11), 1.815(10) 1.897(12), 1.849(11) 1.872(9), 1.910(12) 1.827(10), 1.914(12)
M-D	1.920(8) 1.936(7) , 1.978(8) 1.831(6) 1.909(8)	4× 2.431(2) 4× 2.439(1)	2.596(14) 2.833(15), 2× 3.182(6) 2× 2.840(10), 2× 2.883(11), 2× 2.980(12)	2.325(11), 2.326(9) 2.229(9), 2.340(12) 2.297(9), 2.316(9) 2.199(9), 2.333(11)	M−N	2.213(15) 2.141(16) 2.023(15) 2.024(14)	2.428 (15) 2.582(16) 2.490(15) 2.324(15)	2× 3.141(4), 2× 3.207(4) 2× 3.082(5), 2× 3.139(5)	2.869(16), 3.305(16) 2.832(14), 3.227(14) 2× 3.127(8),	2.505(11), 2.654(10) 2.641(11), 2.627(11) 2.575(8), 2.475(11) 2.758(10)
M-M	3.100(8)	3.779(1)	4.653(15)	4.875(4)	M-M	4.22(2)	4.893(18)	5.77322(8)	5.637(5)	6.432(11)
M-Al	3.214(6) 3.234(5) 3.260(4) 3.328(6) 3.415(6)	4× 3.544(1) 4× 3.779(1)	2× 3.703(9) 4.028(16) 2× 3.815(10) 3.650(16) 4.108(15)	3.754(6), 3.841(7) 3.599(7), 3.578(7) 3.752(6), 3.608(5) 3.732(5), 3.624(5)	M-Al	2.683(16) 3.494(16) 3.449(16)	3.650(17) 3.621(18) 3.601(18) 3.719(17)	2× 3.6336(14) 4.3475(18) 4.7644(19)	3.841(9) 3.437(8) 3.886(8) 2× 4.462(10)	3.218(11) 3.407(10) 3.292(11) 3.882(11)
D-Al-D	110.1(3) 109.2(3) 110.8(3) 108.7(3) 107.1(3) 111.0(3)	4× 107.32(1) 2× 113.86(1)	114.56(72) 111.62(18) 106.15(18) 106.17(23)	112.9(7), 107.5(7) 106.0(7), 107.4(7) 112.8(7), 110.1(8) 110.2(7), 115.4(7) 104.5(8), 112.6(7) 108.3(6), 105.2(6)	N-Al-N	108.4(5) 109.7(2) 121.0(5) 101.2(5) 107.3(3) 107.4(5)	101.3(6) 115.6(6) 99.4(7) 120.4(7) 107.6(7) 110.2(6)	2× 117.2(2) 2× 107.6(2) 103.2(2) 104.7(2)	124.2(8) 2× 103.5(5) 2× 111.3(5) 100.2(6)	107.3(5), 105.8(6) 103.6(5), 110.6(6) 115.6(6), 106.9(6) 113.3(5), 114.5(5) 103.3(5), 107.5(5) 113.9(5), 111.1(6)

Conclusions

In this work, deuterated metal aluminum amides $M[Al(ND_2)_4]_x$ (M = Li, Na, K, Mg and Ca) were successfully synthesized using ball-milling method under liquid ND_3. Previously reported crystal structure models were confirmed with PND and SR-PXD data for $LiAl(ND_2)_4$, $NaAl(ND_2)_4$ and α-$KAl(ND_2)_4$. Rietveld refinements based on PND data revealed that N-H distances in metal aluminum amides have been underestimated and N-D distances of ~1.0 Å were obtained. Structure determination was successful for β-$KAl(ND_2)_4$ (except for D positions) and $Ca[Al(ND_2)_4]_2$. Both structures were built based on the tetrahedral configuration of ND_2^- units around Al atoms. It is observed that the average distances of M-N in $M[Al(ND_2)_4]_x$ is influenced by the ionic radius of the metal. This is in agreement with the trend for M-D distances in $M(AlD_4)_x$ compounds.

Acknowledgements

The EU FP7 Marie Curie Action Incoming International Fellowship project MATERHY (FP7-PEOPLE-2009-IIF, no. 253863) and the FP7 Infrastructure program H2FC are acknowledged for financial support. The authors acknowledge the skillful assistance from the staff of the Swiss-Norwegian Beamline, at the European Synchrotron Radiation Facility, Grenoble, France.

References

[1] Orimo S-i, Nakamori Y, Eliseo JR, Zuettel A, Jensen CM. Complex hydrides for hydrogen storage. Chem Rev. 2007;107:4111-32.

[2] Pukazhselvan D, Kumar V, Singh SK. High capacity hydrogen storage: Basic aspects, new developments and milestones. Nano Energy. 2012;1:566-89.

[3] Srinivasan SS, Brinks HW, Hauback BC, Sun D, Jensen CM. Long term cycling behavior of titanium doped $NaAlH_4$ prepared through solvent mediated milling of NaH and Al with titanium dopant precursors. J Alloys Compd. 2004;377:283-9.

[4] Eymery JB, Truflandier L, Charpentier T, Chotard JN, Tarascon JM, Janot R. Studies of covalent amides for hydrogen storage systems: Structures and bonding of the $MAl(NH_2)_4$ phases with M = Li, Na and K. J Alloys Compd. 2010;503:194-203.

[5] Ono T, Shimoda K, Tsubota M, Hino S, Kojima K, Ichikawa T, et al. Structural and thermal gas desorption properties of metal aluminum amides. J Alloys Compd. 2010;506:297-301.

[6] Chen P, Xiong ZT, Luo JZ, Lin JY, Tan KL. Interaction of hydrogen with metal nitrides and imides. Nature. 2002;420:302-4.

[7] Janot R, Eymery JB, Tarascon JM. Decomposition of $LiAl(NH_2)_4$ and reaction with LiH for a possible reversible hydrogen storage. J Phys Chem C. 2007;111:2335-40.

[8] Rouxel J, Brec R. The amidoaluminate and imidoaluminate of lithium. C R Acad Sci, Ser C. 1966;262:1070-3.

[9] Brec R, Rouxel J. Sodium amidoaluminate and sodium imidoaluminate. C R Acad Sci, Ser C. 1967;264:512-15.

[10] Brec R, Rouxel J. Preparation and X-ray crystallographic study of the potassium, rubidium, and cesium amidoaluminates. Family of alkaline aminoaluminates $MAl(NH_2)_4$. Bull Soc Chim Fr. 1968:2721-6.

[11] Jacobs H, Jaenichen K, Hadenfeldt C, Juza R. Lithium aluminum amide, $LiAl(NH_2)_4$ - preparation, X-ray study, IR spectrum, and thermal decomposition. Z Anorg Allg Chem. 1985;531:125-39.

[12] Jacobs H, Noecker B. Redetermination of structure and properties of the isotypic sodium tetraamidometalates of aluminum and gallium. Z Anorg Allg Chem. 1993;619:381-6.

[13] Molinie P, Brec R, Rouxel J, Herpin P. Structure of sodium, potassium, or cesium tetraamidoaluminate. Structure of sodium tetraamidogallate. Acta Crystallogr, Sect B. 1973;29:925-34.

[14] Jacobs H, Jaenichen K. Preparation and crystal structure of tetraamidoaluminates of rubidium and cesium, $Rb[Al(NH_2)_4]$ and $Cs[Al(NH_2)_4]$. J Less-Common Met. 1990;159:315-25.

[15] Rouxel J, Palvadeau P. Amidoaluminates $SrAl_2(NH_2)_8$ and $BaAl_2(NH_2)_8$. C R Acad Sci, Ser C. 1971;272:63-5.

[16] Pust P, Schmiechen S, Hintze F, Schnick W. Ammonothermal Synthesis and Crystal Structure of $BaAl_2(NH_2)_8 \cdot 2NH_3$. Z Anorg Allg Chem. 2013;639:1185-7.

[17] Brec R, Rouxel J. New type of amidoaluminate: preparation and structural characterization of $Na_2Al(NH_2)_5$. C R Acad Sci, Ser C. 1970;270:491-3.
[18] Palvadeau P, Rouxel J, Charlesworth G, Drew M. Structure of amidoaluminate $CaAl_2(NH_2)_8.NH_3$. C R Acad Sci, Ser C. 1972:881-4.
[19] Palvadeau P, Trelohan AM, Rouxel J. Preparation and structural characterization of calcium amidoaluminate. C R Acad Sci, Ser C. 1969;269:126-8.
[20] Brower FM, Matzek NE, Reigler PF, Rinn HW, Roberts CB, Schmidt DL, et al. Preparation and properties of aluminum-hydride. J Am Chem Soc. 1976;98:2450-3.
[21] Hammersley AP. FIT2D: An Introduction and Overview. ESRF Internal Report1997.
[22] Hauback BC, Fjellvåg H, Steinsvoll O, Johansson K, Buset OT, Jørgensen J. The High Resolution Powder Neutron Diffractometer PUS at the JEEP II Reactor at Kjeller in Norway. J Neutron Res. 2000;8:215-32.
[23] Boultif A, Louer D. Indexing of powder diffraction patterns for low-symmetry lattices by the successive dichotomy method. J Appl Crystallogr. 1991;24:987-93.
[24] Bochu B, Laugier J. Suite of programs for the interpretation of X-ray experiments. LMPG-Suite.
[25] Favre-Nicolin V, Cerny R. FOX, 'free objects for crystallography': a modular approach to ab initio structure determination from powder diffraction. J Appl Crystallogr. 2002;35:734-43.
[26] Favre-Nicolin V, Cerny R. A better FOX: using flexible modelling and maximum likelihood to improve direct-space ab initio structure determination from powder diffraction. Z Kristallogr. 2004;219:847-56.
[27] Larson AC, Von Dreele RB. General Structure Analysis System (GSAS)1994.
[28] Toby BH. J Appl Crystallogr. 2001;34:210-3.
[29] Rietveld HM. Line profiles of neutron powder-diffraction peaks for structure refinement. Acta Crystallogr. 1967;22:151-2.
[30] Rietveld HM. A profile refinement method for nuclear and magnetic structures. J Appl Crystallogr. 1969;2:65-71.
[31] Thompson P, Cox DE, Hastings JB. Rietveld refinement of Debye-Scherrer synchrotron X-ray data from Al_2O_3. J Appl Crystallogr. 1987;20:79-83.
[32] Finger LW, Cox DE, Jephcoat AP. A correction for powder diffraction peak asymmetry due to axial divergence. J Appl Crystallogr. 1994;27:892-900.
[33] Momma K, Izumi F. VESTA 3 for three-dimensional visualization of crystal, volumetric and morphology data. J Appl Crystallogr. 2011;44:1272-6.
[34] Nakamoto K. Theory of Normal Vibrations. Infrared and Raman Spectra of Inorganic and Coordination Compounds: John Wiley & Sons, Inc.; 2008. p. 1-147.
[35] Ono T, Shimoda K, Tsubota M, Kohara S, Ichikawa T, Kojima K, et al. Ammonia Desorption Property and Structural Changes of $LiAl(NH_2)_4$ on Thermal Decomposition. J Phys Chem C. 2011;115:10284-91.

[36] Jacobs H, Juza R. New determination of crystal-structure of lithium amide. Z Anorg Allg Chem. 1972;391:271-9.
[37] Nagib M, Jacobs H. Neutron-diffraction by lithiumdeuteroamide. Atomkernenergie. 1973;21:275-8.
[38] Miwa K, Ohba N, Towata S-i, Nakamori Y, Orimo S-i. First-principles study on lithium amide for hydrogen storage. Phys Rev B. 2005;71:195109.
[39] Hauback BC, Brinks HW, Fjellvåg H. Accurate structure of $LiAlD_4$ studied by combined powder neutron and X-ray diffraction. J Alloys Compd. 2002;346:184-9.
[40] Hauback BC, Brinks HW, Jensen CM, Murphy K, Maeland AJ. Neutron diffraction structure determination of $NaAlD_4$. J Alloys Compd. 2003;358:142-5.
[41] Hauback BC. Structures of aluminium-based light weight hydrides. Z Kristallogr. 2008;223:636-48.
[42] Sato T, Sørby MH, Ikeda K, Sato S, Hauback BC, Orimo S. Syntheses, crystal structures, and thermal analyses of solvent-free $Ca(AlD_4)_2$ and $CaAlD_5$. J Alloys Compd. 2009;487:472-8.
[43] Shannon RD. Revised effective ionic-radii and systematic studies of interatomic distances in halides and chalcogenides. Acta Crystallogr Section A. 1976;32:751-67.
[44] Hauback BC, Brinks HW, Heyn RH, Blom R, Fjellvåg H. The crystal structure of $KAlD_4$. J Alloys Compd. 2005;394:35-8.

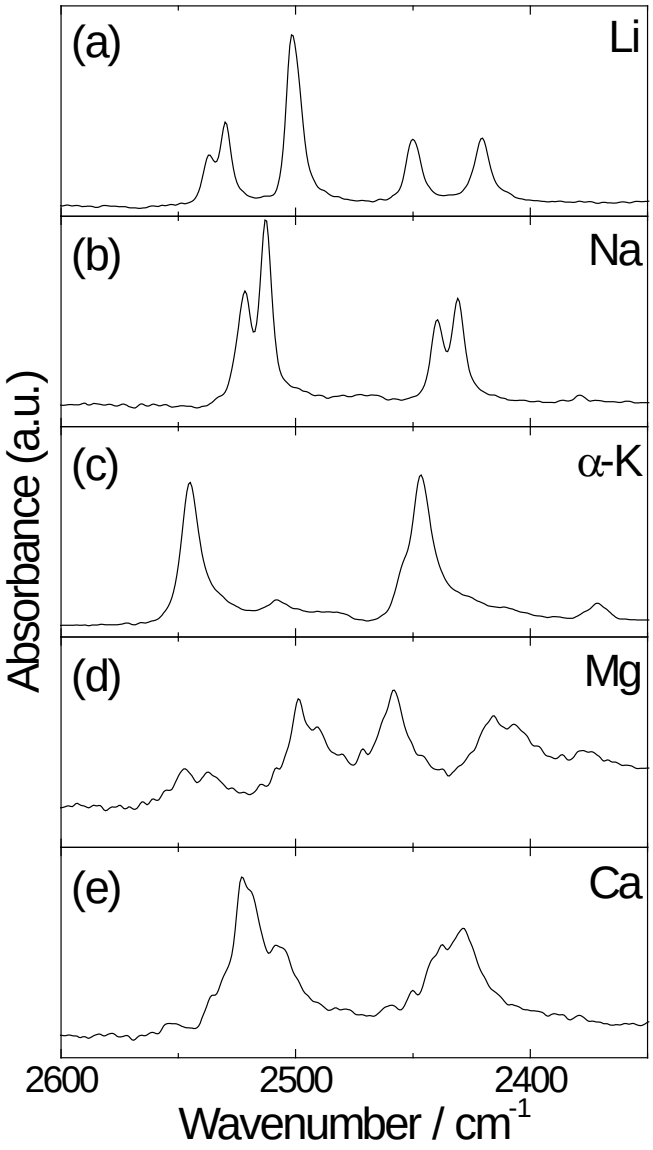

Fig. 1. ATR-IR spectra of N-D stretching region for: (a) $LiAl(ND_2)_4$, (b) $NaAl(ND_2)_4$, (c) α-$KAl(ND_2)_4$, (d) $Mg[Al(ND_2)_4]_2$ and (e) $Ca[Al(ND_2)_4]_2$. All spectra were recorded under an Ar atmosphere at RT.

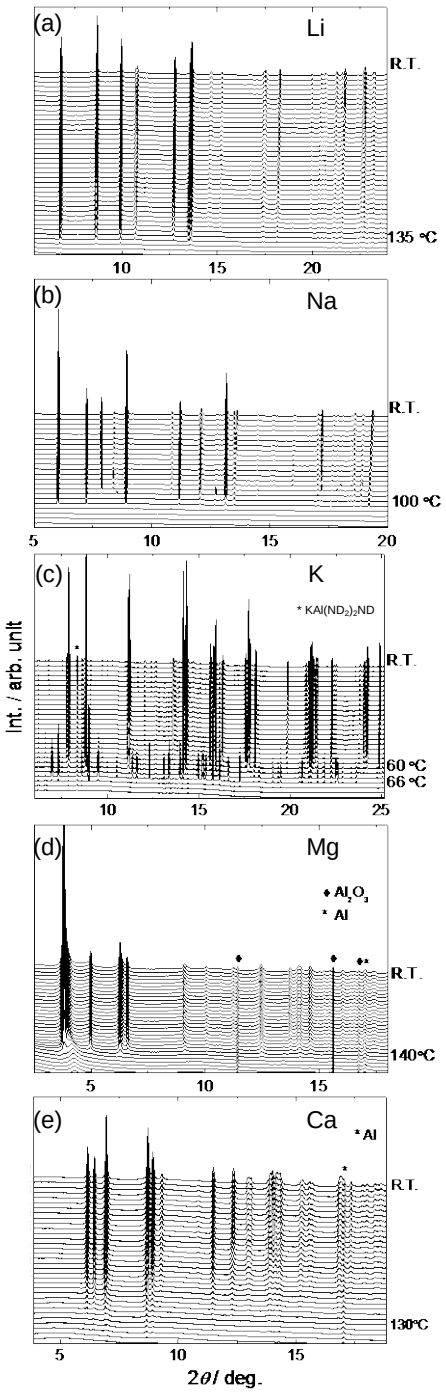

Fig.2. *In-situ* SR-PXD data for (a) $LiAl(ND_2)_4$, (b) $NaAl(ND_2)_4$, (c) $KAl(ND_2)_4$, (d) $Mg[Al(ND_2)_4]_2$ and (e) $Ca[Al(ND_2)_4]_2$ with λ = 0.693862 Å. The heating rate was 2 (c) or 5 °C/min (the others). A diffraction profile was collected every 40 s.

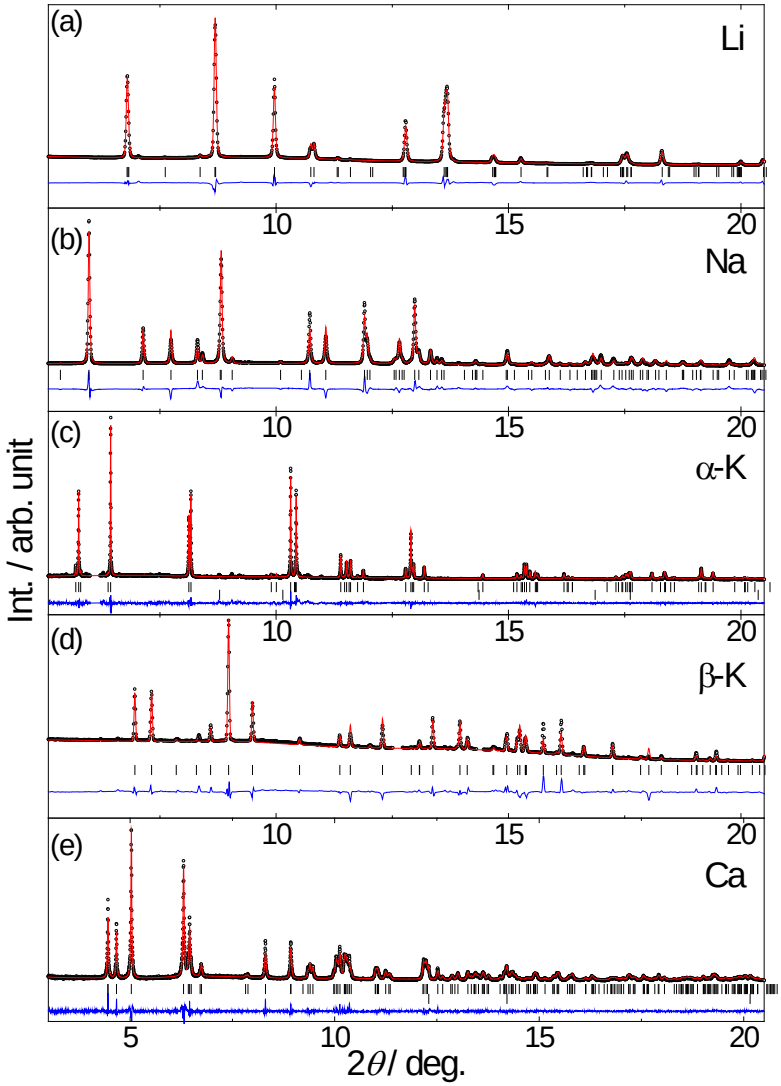

Fig.3. Rietveld refinement of the SR-PXD patterns of: (a) $LiAl(ND_2)_4$ with λ = 0.693862 Å, (b) $NaAl(ND_2)_4$ with λ = 0.68291 Å, (c) α-$KAl(ND_2)_4$ with λ = 0.50462 Å, the region from 6.00 to 6.21º was excluded because of the reflection from the partially decomposed product $KAl(ND_2)_2ND$. (d) β-$KAl(ND_2)_4$ with λ = 0.693862 Å, (e) $Ca[Al(ND_2)_4]_2$ with λ = 0.50123 Å. The black dot, red and blue lines are the observed, calculated and difference between observed and calculated patterns, respectively. The positions of the Bragg peaks are shown by the ticks. In Fig. 4c upper ticks are from α-$KAl(ND_2)_4$ and lower from unreacted KH, and in Fig. 4e, upper ones from $Ca[Al(ND_2)_4]_2$ and lower from unreacted Al phase.

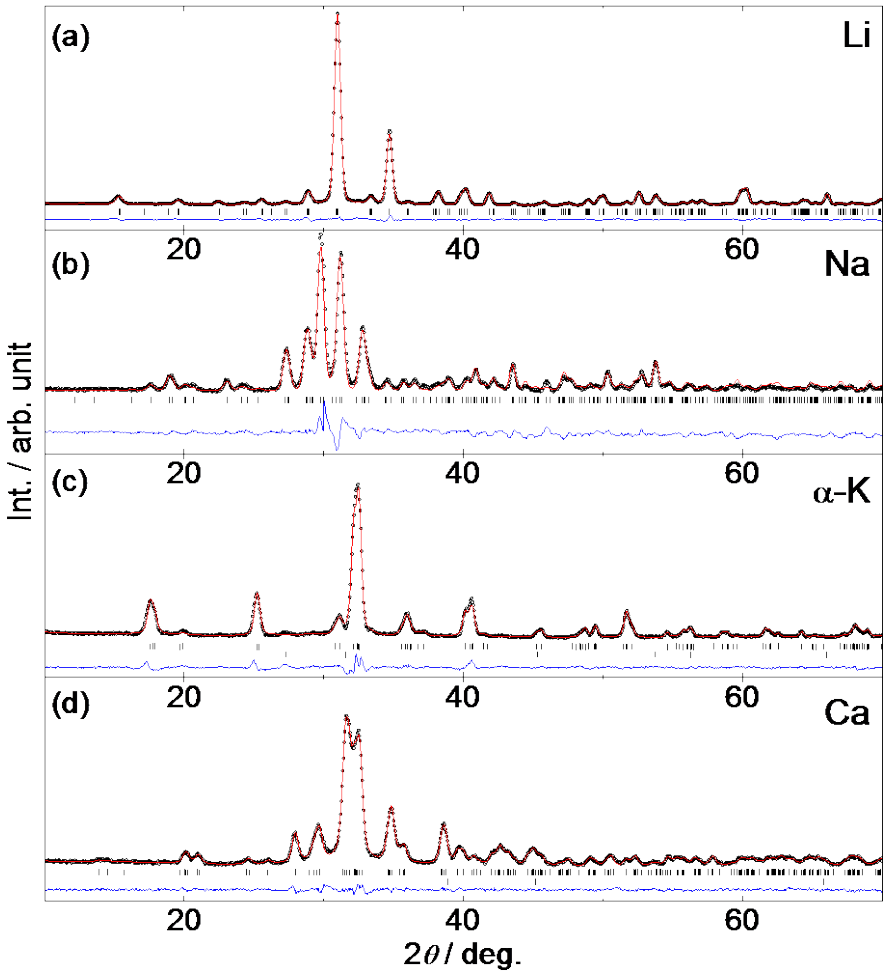

Fig.4. Rietveld refinement of the PND patterns of: (a) $LiAl(ND_2)_4$, (b) $NaAl(ND_2)_4$, (c) α-$KAl(ND_2)_4$, (d) $Ca[Al(ND_2)_4]_2$ with λ = 1.5556 Å. The black dot, red and blue lines are the observed, calculated and difference between experimental and calculated pattern, respectively. The positions of the Bragg peaks are shown by the ticks. In Fig. 5c upper ticks are from α-$KAl(ND_2)_4$ and lower from unreacted KH, and in Fig. 5d, upper ones from $Ca[Al(ND_2)_4]_2$ and lower from unreacted Al phase.

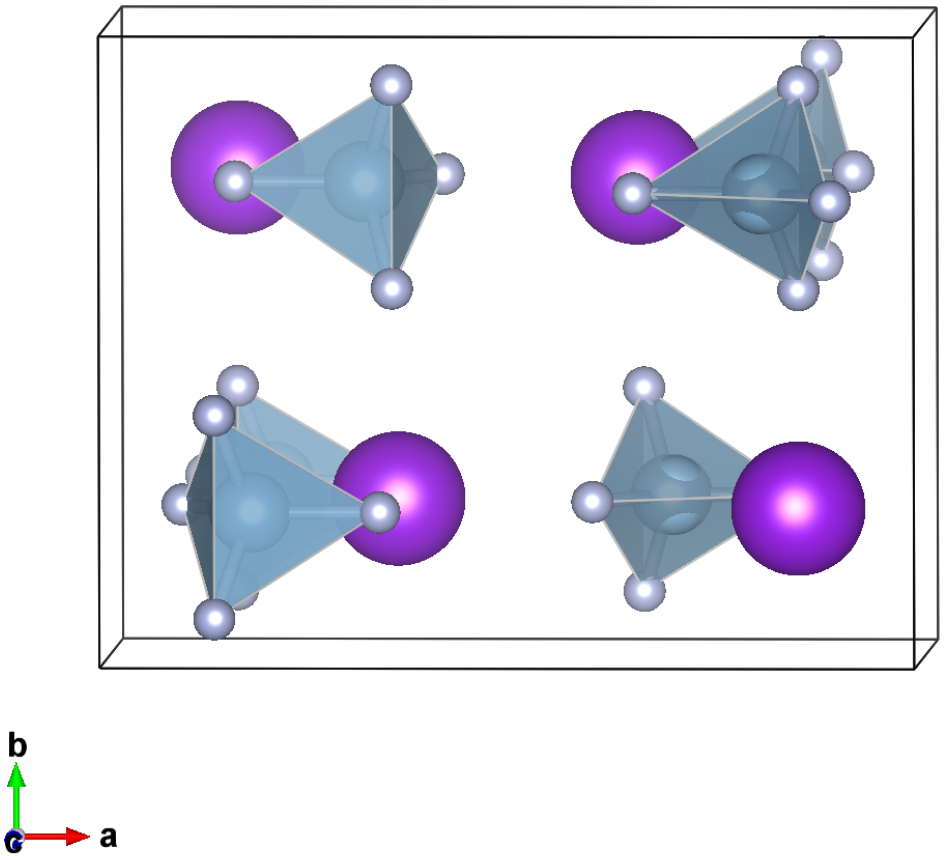

Fig. 5. Visualization of the crystal structure of β-$KAl(ND_2)_4$. K: purple spheres, Al: in centers of blue tetrahedra, N: gray spheres.

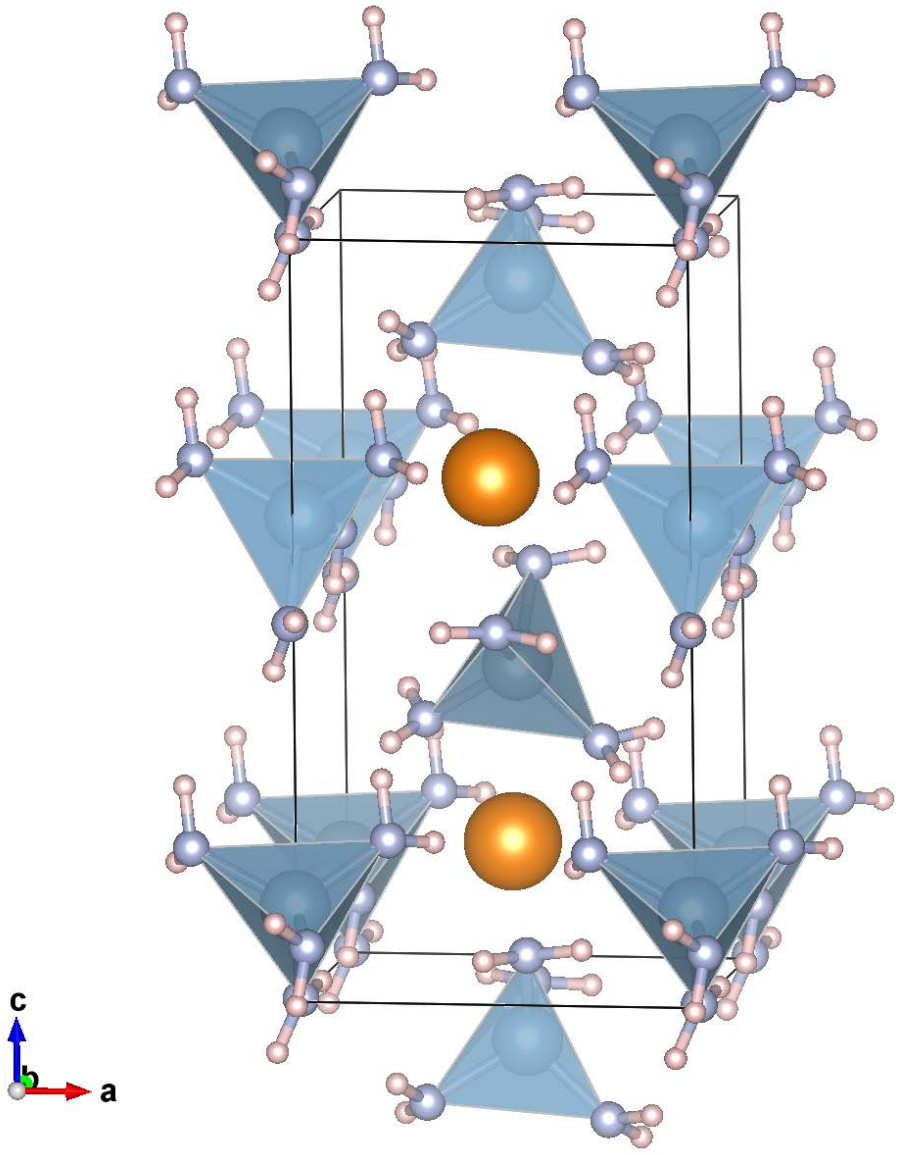

Fig.6. Visualization of the crystal structure of $Ca[Al(ND_2)_4]_2$. Ca: orange spheres, Al: in centers of blue tetrahedra, N: gray spheres, D: pink spheres.

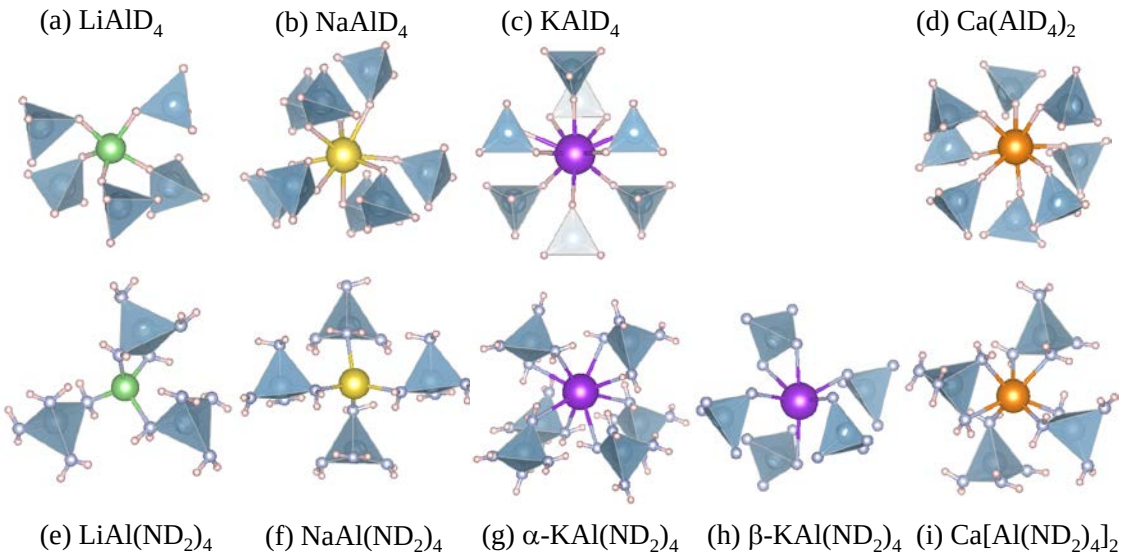

Fig.7. Coordination of metal atoms to AlD_4/AlN_4 tetrahedra in $M(AlD_4)_x/M[Al(ND_2)_4]_x$. Al: in centers of blue tetrahedra, D: pink, N: gray, Li: green (a, e), Na: yellow (b, f), K: purple (c, g, h) and Ca: orange spheres (d, i).

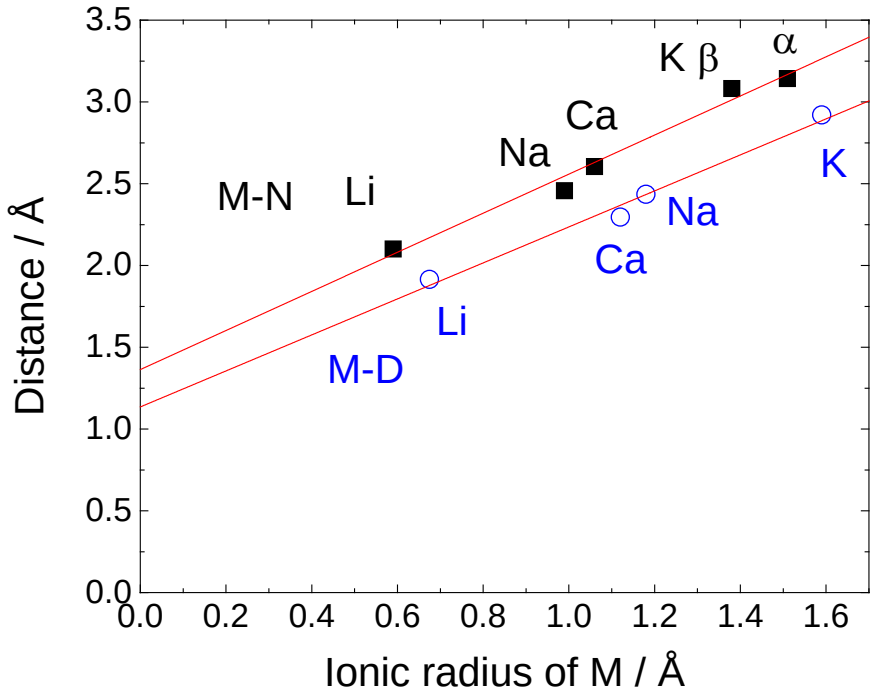

Fig. 8. A comparison of averaged M-N distances in $M[Al(ND_2)_4]_x$ and M-D distances in $M(AlD_4)_x$ as a function of effective ionic radii of metals together with linear fits.